

Comparison of Embedded Cluster Models to Study Zeolite Catalysis: Proton Transfer Reactions in Acidic Chabazite

STEPHEN P. GREATBANKS,¹ IAN H. HILLIER,^{1*}
and PAUL SHERWOOD²

¹Department of Chemistry, University of Manchester, Oxford Road, Manchester M13 9PL, UK

²CLRC Daresbury Laboratory, Daresbury, Warrington, UK

Received 6 June 1996; accepted 27 June 1996

ABSTRACT

A number of cluster models used to study the interaction of NH_3 and NH_4^+ with the Brønsted sites of the acidic zeolite, chabazite, are assessed by comparison with the results from full periodic Hartree–Fock calculations. Corrections to bare cluster models to take account of the electrostatic environment due to the periodic zeolite are found to agree well with periodic calculations, and appear to be more successful than a more sophisticated embedding procedure. © 1997 by John Wiley & Sons, Inc.

Introduction

The accurate modeling of proton transfer reactions within zeolite pore systems is vital in helping to discern the mechanisms by which a number of important reactions are catalyzed.¹ It has been established that the presence of acidic Brønsted sites, comprised of bridging hydroxyl groups neighboring aluminum substitution sites,

are central to these reactions, and much experimental^{2–4} and theoretical^{4–9} work has been carried out to determine the manner of their interaction with basic substrate molecules. At present, there is a degree of uncertainty regarding the ability of zeolite Brønsted acidic sites to protonate basic substrates, with H_2O , CH_3OH , and NH_3 most often being considered. While the situation with H_2O and CH_3OH is still somewhat uncertain^{7,10–13} with evidence for both neutral and protonated substrates, it is generally acknowledged that NH_3 is sufficiently basic to be protonated at a Brønsted site to give NH_4^+ .¹⁴ For this reason, the

* Author to whom all correspondence should be addressed.

$\text{NH}_3/\text{NH}_4^+$ system is a suitable candidate for the comparison and calibration of different theoretical methods.

While it has been traditional to investigate zeolite–substrate interactions using bare cluster models,^{15,16} recent studies have recognized the importance of including more features of the periodic zeolite to properly model the subtle, yet potentially chemically important, aspects of the substrate active-site interaction. In particular, a range of more sophisticated models has been developed to include a realistic representation of the long-range electrostatic influence of the zeolite framework. A number of approaches have been suggested which can vary substantially in complexity, yet all are essentially embedded cluster models.

The most simple, from a conceptual and computational viewpoint, are the so-called cluster-in-crystal-field (CICF) approaches in which the effect of the extended zeolite is incorporated as a perturbation to the cluster Hamiltonian via point charges, implemented by a number of workers.^{17–20} In more sophisticated variants of this method Teunissen et al.^{19,21} and Greatbanks et al.²² have utilized periodic Hartree–Fock calculations to construct a potential within which the cluster is embedded. Perhaps the most sophisticated of the embedded cluster methods uses Green function techniques to self-consistently generate a potential within which the region of chemical interest is embedded. More specifically, this model, implemented within the code EMBED,²³ is a perturbed cluster (PC) approach in which the region of interest (the defect) is described using a molecular cluster, with corrective terms (expressed in terms of the density of states (DOS) of the perfect crystal wave function, obtained using the same computational technique as that used for the defect) included to ensure correct coupling of the cluster to the complementary region. Such an approach allows for charge transfer across the boundary of the cluster, but necessarily requires that the perturbation in the DOS due to the defect is small.²⁴

It is important to judge the value of these different approaches, which can be carried out by comparison with full periodic calculations employing a supercell of sufficient size to minimize intersubstrate interactions between adjacent cells. We adopt such an approach in this study by comparing the results of a series of minimal basis set calculations. Our objective is thus not to model substrate–zeolite interactions to a chemical accuracy, but rather to compare the results of a range of embedding procedures.

Computational Details

For the current study, the interaction of NH_3 and NH_4^+ substrates with acidic chabazite was considered. We chose this system because it has been the subject of both an embedding procedure designed to correct for the long-range electrostatic potential of the crystal and the embedding method of Pisani and coworkers. The zeolite geometry used was that resulting from energy minimization within the shell model of the acidic aluminosilicate, using the parameters of Schröder,^{25,26} with an Si:Al ratio of 3, chosen to allow comparison with previous studies.^{19,27} The cluster selected, shown in Figure 1, includes half of the characteristic 8-ring and has stoichiometry $\text{Si}_2\text{Al}_2\text{O}_{13}\text{H}_{12}$ with dangling bonds saturated by hydrogens, giving an OH bond length of 1.00 Å along the broken bond vector. This is intermediate between the small (cluster II, SiAlO_7H_7) and medium (cluster I, $\text{Si}_6\text{Al}_2\text{O}_{10}\text{H}_{16}$) clusters used by Teunissen et al.,¹⁹ and somewhat larger than the clusters used by Pisani²⁷ (SiAlO_7H and SiAlO_8H). All calculations were carried out using an STO-3G basis.

We here compare the results of our embedding method with the results of Teunissen et al.¹⁹ and Pisani and Birkenheuer.²⁷ We have previously described²² our procedure to obtain potential derived charges (PDC) to provide a realistic electrostatic environment for the cluster. Briefly, a periodic Hartree–Fock calculation of the acidic zeolite is carried out (via the code CRYSTAL 92²⁸) to generate an electrostatic potential. A fitting procedure is then used to generate a set of PDC so that the potential due to the cluster, with appropriate termination of dangling bonds, combined with that of the PDC, reproduces the potential from the full periodic calculation.

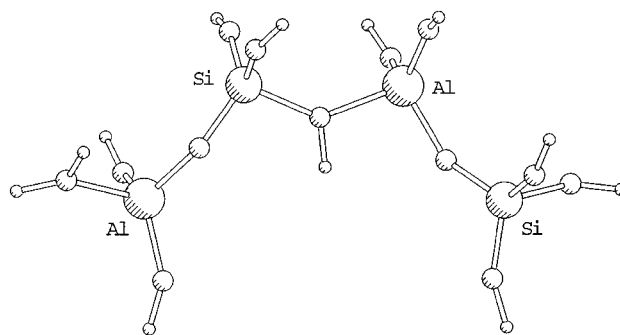


FIGURE 1. Acidic cluster $\text{Si}_2\text{Al}_2\text{O}_{13}\text{H}_{12}$.

For the purpose of comparison, the interaction of NH_3 and NH_4^+ (fixed at their respective experimental geometries^{29,30}), with the neutral and anionic forms of the acidic chabazite, respectively, was considered (see Figs. 2 and 3). The structure of the anionic form was assumed to be the same as that of the neutral species, thus ignoring the important effect of cluster relaxation upon proton transfer. The potential energy surfaces were generated by variation of the N—O distance while maintaining the coincidence of the NH_3 and NH_4^+ symmetry axes with the OH axis, thus allowing comparison of the relative merits of the embedded cluster model of Pisani (EMBED) and the cluster-in-crystal-field approaches of Teunissen (CICF) and ourselves (PDC), using periodic supercell calculations (SC)²⁸ as benchmarks. Within the supercell calculations, there exists the possibility of including either one or three substrate molecules within the unit cell.²¹ As our PDC model, and embedded cluster models in general, are designed to consider substrates interacting within the so-called “dilute approximation,” we have chosen to include a single substrate within the unit cell. A second comparison was performed, in which the zeolitic Brønsted proton transfers from the zeolite to NH_3 , forming NH_4^+ according to the reaction path suggested by Pisani and Birkenheuer.²⁷ In their study, if the distance of the acidic proton (H^B) from the acidic oxygen (O^B) is close to its equilibrium value, the structure of NH_3 was taken to be that of the free base, while as, if proton transfer had largely occurred, the structure of NH_4^+ was taken. For intermediate cases, both structures of NH_3 were considered. We note again that all atoms of the zeolite cluster, with the exception of the acidic proton noted previously, were held fixed at the periodic geometry. The third comparison involved modeling the interaction of the zeolite with $\text{NH}_3/\text{NH}_4^+$ in the presence of water that was hydrogen bonded to the substrate. Appropriate structures were again provided by Pisani and Birkenheuer.

The embedded cluster calculations were performed using the code GAMESS-UK.³¹

Computational Results

We first consider the interaction of fixed geometry NH_3 and NH_4^+ with the zeolite acid site geometry. In Figure 4 we show the calculated potential energy curves for this interaction. Here, and in

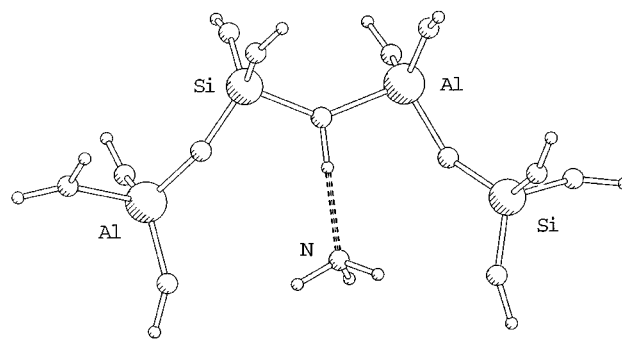


FIGURE 2. Acidic cluster + NH_3 .

future discussion, we define the binding energy as:

$$E_{\text{binding}} = E_{\text{chabazite} + \text{NH}_3} - E_{\text{chabazite}} - E_{\text{NH}_3}$$

where $E_{\text{chabazite} + \text{NH}_3}$ is the energy of the zeolite system (cluster or periodic) containing the substrate, $E_{\text{chabazite}}$ is the energy of the acidic zeolite (again, cluster or periodic), and E_{NH_3} is the energy of isolated NH_3 in the gas phase. It can be seen that the simpler embedded cluster models (CICF with an $\text{Si}_6\text{Al}_2\text{O}_{10}\text{H}_{16}$ cluster and PDC using an $\text{Si}_2\text{Al}_2\text{O}_{13}\text{H}_{12}$ cluster) predict binding energies (and substrate–zeolite distances) close to the supercell values. The EMBED method, although also giving accurate structures, somewhat overestimates the binding energy. The binding energies also suggest that the PDC method provides an interaction energy somewhat more accurate than that from both medium ($\text{Si}_6\text{Al}_2\text{O}_{10}\text{H}_{16}$) and large ($\text{Si}_{10}\text{Al}_2\text{O}_{26}\text{H}_{24}$) sized clusters within the CICF model. An interesting feature of these comparative calculations (Fig. 4) is that both CICF and PDC embedding procedures result in an increase in

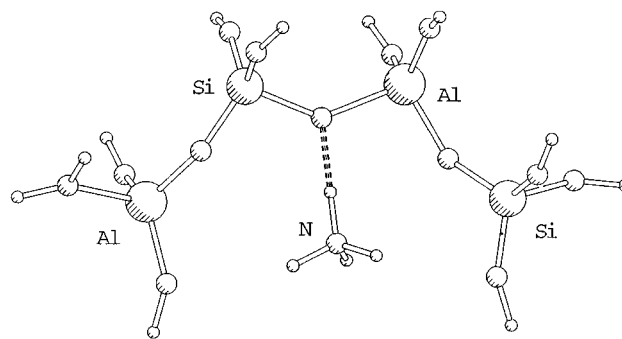


FIGURE 3. Anionic cluster + NH_4^+ .

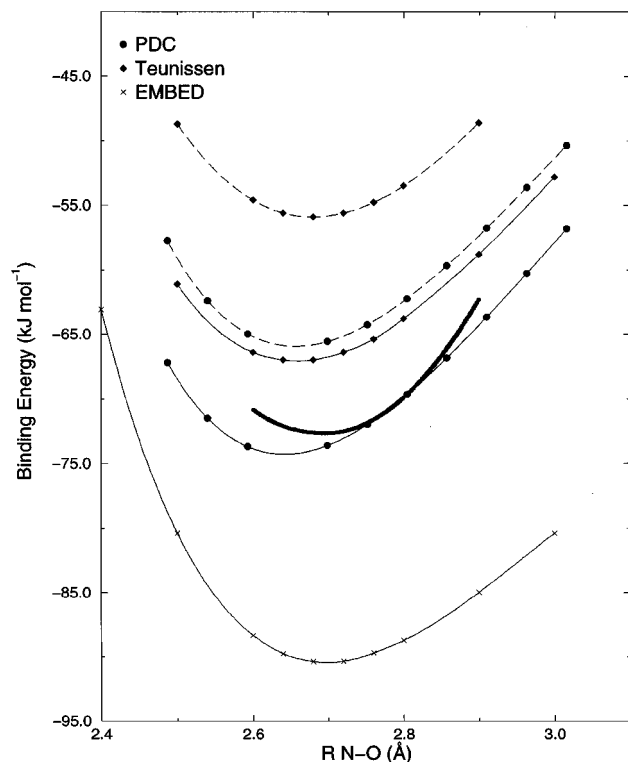


FIGURE 4. Potential energy curves for the interaction of fixed NH_3 with the Brønsted proton of acidic chabazite. The heavy line indicates the supercell result. Dashed lines indicate the corresponding bare cluster calculations ($\text{Si}_6\text{Al}_2\text{O}_{10}\text{H}_{16}$ and $\text{Si}_2\text{Al}_2\text{O}_{13}\text{H}_{12}$ for the CICF method of Teunissen and our PDC method, respectively).

binding energy of $\sim 10 \text{ kJ mol}^{-1}$ compared to the bare cluster result, demonstrating a stabilizing influence from the bulk zeolite. A similar trend is found in the case of the interaction of NH_4^+

(Fig. 5), where both PDC and CICF procedures provide results which are comparable, although the PDC model tends to underestimate the binding energy by $\sim 6 \text{ kJ mol}^{-1}$, with the CICF method overestimating by a similar amount. Again, while the N—O distances corresponding to minima in the NH_4^+ binding energy curves are well reproduced by the EMBED method, there seems to be some tendency to “overbind” the substrate. For all procedures, the effect of the embedding is again to provide a stabilization of the docked substrate.

We turn now to the $\text{NH}_3/\text{NH}_4^+$ proton transfer reaction. The energetics of the transfer of the acidic proton from the Brønsted acidic site of chabazite to NH_3 for structures along the path³² have been determined in a previous study,²⁷ for two different clusters, $\text{O}_3\text{Al}(\text{OH})\text{SiO}_3$ and $\text{O} + \text{O}_3\text{Al}(\text{OH})\text{SiO}_3$, the larger of these clusters incorporating an additional oxygen atom at the far side of the zeolite 8-ring.²⁷ Periodic supercell calculations have been performed by us at structures along this path as a reference for comparison of the PDC and EMBED methods. The potential energy surfaces for the interaction of NH_3 and NH_4^+ with the zeolitic acid site, where the hydrogen of the Brønsted acidic site is permitted to transfer, are shown in Figure 6. It is clear that the binding energies for the various methods differ considerably in the NH_4^+ regime (reaction coordinates $> 0 \text{ Å}$). When the reaction coordinate is $\sim 0.5 \text{ Å}$, the calculated interaction energy of the PDC embedded cluster differs by ~ 100 and $\sim 200 \text{ kJ mol}^{-1}$ compared to the EMBED calculations using the larger $[\text{O} + \text{O}_3\text{Al}(\text{OH})\text{SiO}_3]$ and smaller $[\text{O}_3\text{Al}(\text{OH})\text{SiO}_3]$ clusters, respectively.

TABLE I.

Comparison of Binding Energies, E_{binding} (kJ mol^{-1}), Equilibrium N—O^B Distances, d_{eq} (Å), and Energies of Proton Transfer, $\Delta E = E_{\text{binding}}(\text{NH}_4^+) - E_{\text{binding}}(\text{NH}_3)$ (kJ mol^{-1}), for Different Theoretical Approaches.

	SC ^a	EMBED ^b	PDC ^c	CICF ^d	CICF ^e	CICF ^f
$E_{\text{binding}}(\text{NH}_3)$	-72	-90	-74	-118	-68	-65
$d_{\text{eq}}(\text{NH}_3)$	2.72	2.70	2.64	2.59	2.66	2.69
$E_{\text{binding}}(\text{NH}_4^+)$	117	102	111	25	123	124
$d_{\text{eq}}(\text{NH}_4^+)$	2.25	2.29	2.26	2.26	2.24	2.22
ΔE	189	192	185	143	191	189

^a Periodic.

^b SiAlO_7H .²⁷

^c $\text{Si}_2\text{Al}_2\text{O}_{12}\text{H}_{13}$.²²

^d SiAlO_7H_7 .^{19, 21}

^e $\text{Si}_6\text{Al}_2\text{O}_{10}\text{H}_{16}$.^{19, 21}

^f $\text{Si}_{10}\text{Al}_2\text{O}_{26}\text{H}_{24}$.^{19, 21}

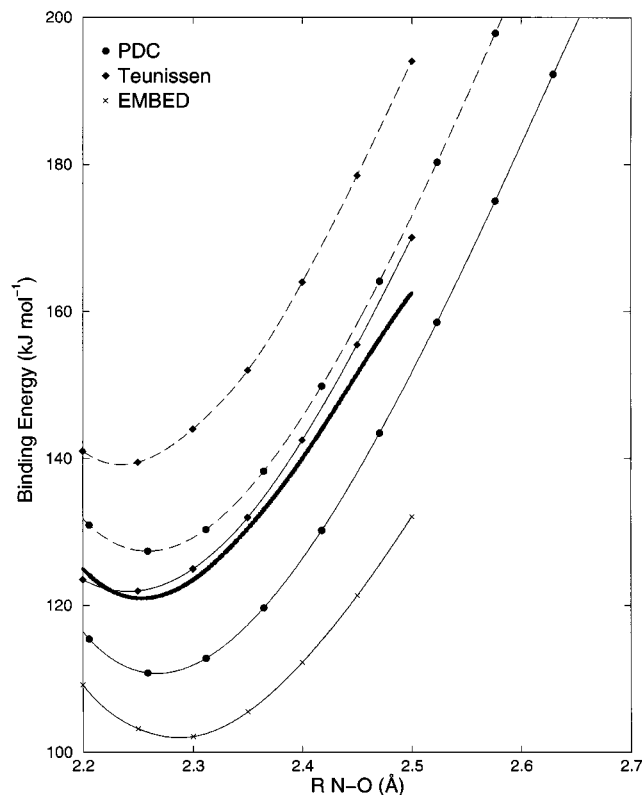


FIGURE 5. Potential energy curves for the interaction of fixed NH_4^+ with the Brønsted proton of acidic chabazite. The heavy line indicates the supercell result. Dashed lines indicate the corresponding bare cluster calculations ($\text{Si}_6\text{Al}_2\text{O}_{10}\text{H}_{16}$ and $\text{Si}_2\text{Al}_2\text{O}_{13}\text{H}_{12}$ for the CICF method of Teunissen and our PDC method, respectively).

Our final model system involves the effect of coadsorbed water on the $\text{NH}_3/\text{NH}_4^+$ proton transfer reaction. The effect of allowing a water molecule to interact with the substrate is, as expected, to preferentially stabilize the ionic (NH_4^+) species. The effect is reproduced by all models considered (Fig. 7). However, this effect is considerably larger for the EMBED calculations. Thus, the addition of H_2O results in a large stabilization ($\sim 600 \text{ kJ mol}^{-1}$) of the protonated base (values of the reaction coordinate close to 1 Å) with the PDC model predicting a smaller effect. The effect of increasing the size of the cluster within EMBED, by inclusion of an extra oxygen at the far side of the 8-ring, is to reduce the degree of stabilization. The bare cluster results, also included in Figure 7, show that, for values of the reaction coordinate between -3 and -1 Å , this model well reproduces the supercell result, although the PDC embedding procedure is required to model the proton transfer correctly, as

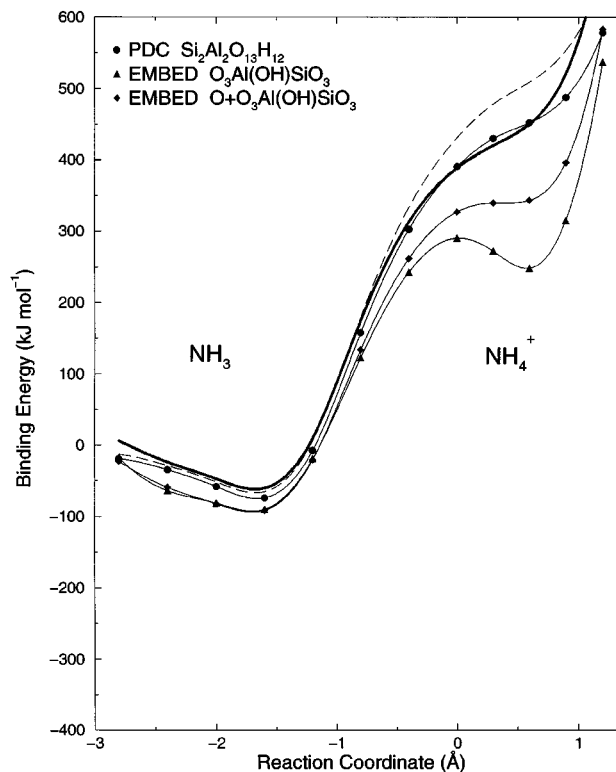


FIGURE 6. Proton transfer reaction potential energy curves for the interaction of $\text{NH}_3 / \text{NH}_4^+$ with the Brønsted proton of the acidic chabazite. The dashed line indicates the bare $\text{Si}_2\text{Al}_2\text{O}_{13}\text{H}_{12}$ cluster. The heavy line indicates the supercell result.

greater deviations are observed at larger values of the reaction coordinate.

Discussion

In this article, we have presented a comparison between some alternative procedures currently employed to model the often complex interaction between simple substrates and zeolite active sites. Although full periodic calculations are now feasible using methods evolved from the area of molecular ab initio structure calculations (CRYSTAL)²⁸ and from plane-wave/density functional methods of solid state physics,^{13,33} methods that are more computationally economic are certainly needed. It is clear that quite simple schemes, employing an electrostatic correction to bare cluster models, are very effective. This is not unexpected in view of the partially ionic nature of zeolites. Such models may be further developed by use of more realistic models of the solid environment by including a more precise description of the rest of the zeolite

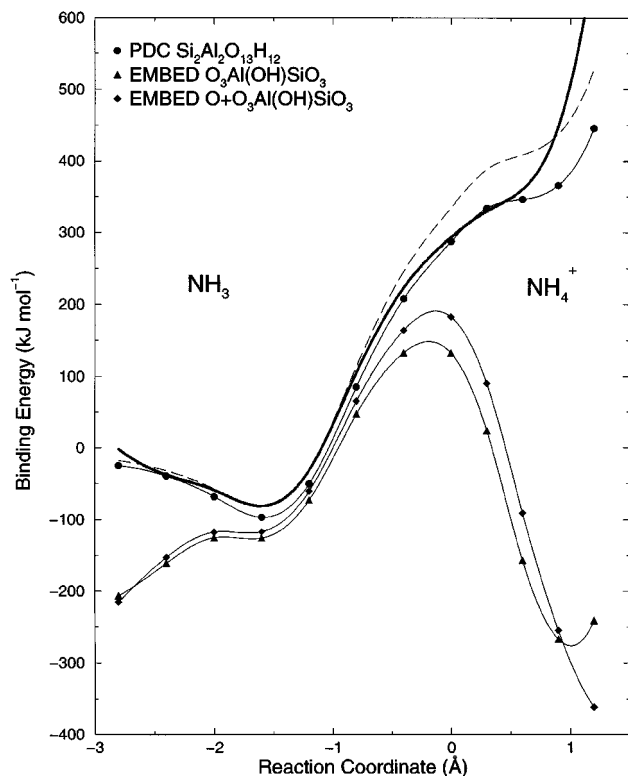


FIGURE 7. Proton transfer reaction path potential energy curves for the interaction of $\text{NH}_3/\text{NH}_4^+$ and coadsorbed H_2O , with the Brønsted proton of the acidic chabazite. The dashed line indicates the bare $\text{Si}_2\text{Al}_2\text{O}_{13}\text{H}_{12}$ cluster. The heavy line indicates the supercell result.

beyond a simple monopole model, to more completely reflect its actual electronic structure. One such approach along these lines is exemplified by the EMBED calculations discussed in this article. However, we find the somewhat unexpected result that this approach, in its present form, does not result in an improved description, and indicates an overestimation of the interaction with the zeolite. The origin of this effect is not clear. It may be significant that the greatest effects are found when the substrate is approaching the zeolite frame, where charge transfer may occur. This effect may be responsible for the observation that, in the case of the $\text{NH}_3/\text{NH}_4^+$ proton transfer model (Fig. 6), increasing the size of the cluster within the EMBED model improves the agreement with the supercell calculation while this is not found for the reaction involving coadsorbed H_2O (Fig. 7). Here such charge transfer may occur more readily, because the water molecule is closer to the zeolite frame. Clearly, further studies are needed to resolve this problem.

Acknowledgments

We thank EPSRC for support of this research, and Professor Pisani and Dr. Birkenheuer for their data and helpful discussion.

References

1. H. van Bekkum, E. M. Flanigen, and J. C. Jansen, *Introduction to Zeolite Science and Practice*, Elsevier, Amsterdam, 1991.
2. L. M. Parker, D. M. Bibby, and G. R. Burns, *Zeolites* **11**, 293 (1991).
3. A. Jentys, G. Warecka, M. Derewinski, and J. Lercher, *J. Phys. Chem.*, **93**, 4837 (1989).
4. J. Sauer, P. Ugliengo, E. Garrone, and V. R. Saunders, *Chem. Rev.*, **94**, 2095 (1994).
5. J. Sauer, H. Horn, M. Häser, and R. Ahlrichs, *Chem. Phys. Lett.*, **173**, 26 (1990).
6. E. Kassab, K. Seiti, and M. Allavena, *J. Phys. Chem.*, **95**, 9425 (1991).
7. J. D. Gale, C. R. A. Catlow, and J. R. Carruthers, *Chem. Phys. Lett.*, **216**, 155 (1993).
8. S. Bates and J. Dwyer, *J. Mol. Struct. (Theochem)*, **306**, 57 (1994).
9. R. A. van Santen and G. J. Kramer, *Chem. Rev.*, **95**, 637 (1995).
10. F. Haase and J. Sauer, *J. Am. Chem. Soc.*, **117**, 3780 (1995).
11. J. Sauer, *Science*, **271**, 774 (1996).
12. L. Smith, A. K. Cheetham, R. E. Morris, L. Marchese, J. M. Thomas, P. A. Wright, and J. Chen, *Science*, **271**, 799 (1996).
13. R. Shah, M. C. Payne, M.-H. Lee, and J. D. Gale, *Science*, **271**, 1395 (1996).
14. S. P. Greatbanks, P. Sherwood, I. H. Hillier, R. J. Hall, N. A. Burton, and I. R. Gould, *Chem. Phys. Lett.*, **234**, 367 (1995).
15. E. H. Teunissen, F. B. van Duijneveldt, and R. A. van Santen, *J. Phys. Chem.*, **96**, 366 (1992).
16. E. H. Teunissen, R. A. van Santen, A. P. J. Jansen, and F. B. van Duijneveldt, *J. Phys. Chem.*, **97**, 203 (1993).
17. R. Vetrivel, C. R. A. Catlow, and E. A. Colbourn, *Proc. R. Soc. Lond. A* **417**, 81 (1988).
18. R. Vetrivel, C. R. A. Catlow, and E. A. Colbourn, *J. Phys. Chem.*, **93**, 4597 (1989).
19. E. H. Teunissen, A. P. J. Jansen, R. A. van Santen, R. Orlando, and R. Dovesi, *J. Chem. Phys.*, **101**, 5865 (1994).
20. A. Kyrilidis, S. J. Cook, A. K. Chakraborty, A. T. Bell, and D. N. Theodorou, *J. Phys. Chem.*, **99**, 1505 (1995).
21. E. H. Teunissen, C. Roetti, C. Pisani, A. J. M. de Man, A. P. J. Jansen, R. Orlando, R. A. van Santen, and R. Dovesi, *Model. Simul. Mater. Sci. Eng.*, **2**, 921 (1994).
22. S. P. Greatbanks, P. Sherwood, and I. H. Hillier, *J. Phys. Chem.*, **98**, 8134 (1994).
23. C. Pisani, F. Corà, R. Nada, and R. Orlando, *EMBED 93 User Documentation*, University of Torino, 1993.

24. C. Pisani, R. Dovesi, R. Nada, and L. N. Kantorovich, *J. Chem. Phys.*, **92**, 7448 (1990).
25. K-P. Schröder, J. Sauer, M. Leslie, C. R. A. Catlow, and J. M. Thomas, *Chem. Phys. Lett.*, **188**, 320 (1992).
26. K-P. Schröder, J. Sauer, M. Leslie, and C. R. A. Catlow, *Zeolites*, **12**, 20 (1992).
27. C. Pisani and U. Birkenheuer, *Int. J. Quant. Chem.*, **S29**, 221 (1995).
28. R. Dovesi, V. R. Saunders, and C. Roetti, *Crystal 92 User Documentation*, University of Torino, 1992.
29. G. Herzberg, *Molecular Spectra and Molecular Structure*, Vol. 2, Van Nostrand, Princeton, NJ, 1945.
30. J. A. Ibers and D. P. Stevenson, *J. Chem. Phys.*, **28**, 929 (1958).
31. GAMESS-UK is a package of *ab initio* programs written by M. F. Guest, J. H. van Lenthe, J. Kendrick, K. Schoffel, P. Sherwood, and R. J. Harrison, with contributions from R. D. Amos, R. J. Buenker, M. Dupuis, N. C. Handy, I. H. Hillier, P. J. Knowles, V. Bonacic-Koutecky, W. von Niessen, V. R. Saunders, and A. J. Stone. The package is derived from the original GAMESS code from M. Dupuis, D. Spangler, and J. Wendolowski, *NRCC Software Catalog*, Vol. 1, Program No. QG01, GAMESS, 1980.
32. U. Birkenheuer (personal communication).
33. E. Nusterer, P. E. Blöchl, and K. Schwarz, *Angewandte Chemie Int. Ed.*, **108**, 187 (1996).